

Expanded View Figures

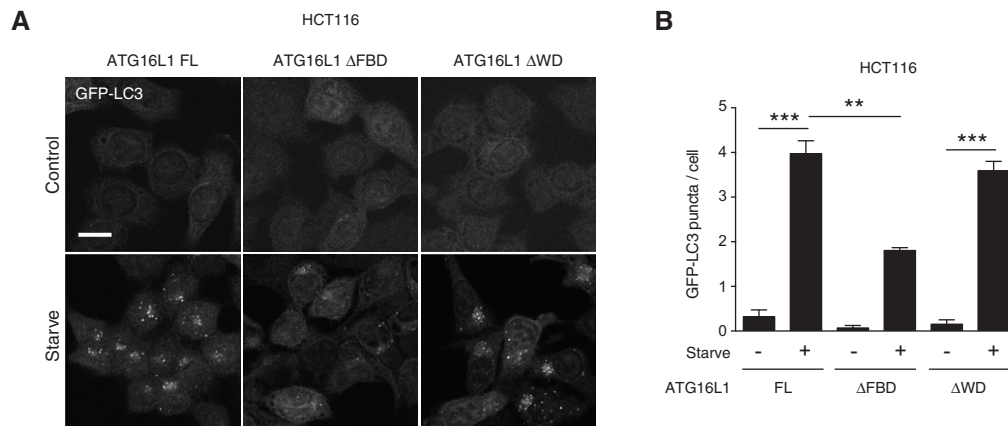


Figure EV1. The WD40 CTD of ATG16L1 is not required for canonical autophagy.

A Confocal images of GFP-LC3-expressing HCT116 *ATG16L1*^{-/-} complemented with full-length (FL), Δ FBD or Δ WD ATG16L1 under fed or starvation conditions. Scale bar: 10 μ m.

B Quantification of GFP-LC3 puncta in ATG16L1-complemented HCT116 cells under fed or starvation conditions.

Data information: In (B), data are presented as mean \pm SEM from three independent experiments. ****P* < 0.0004, ***P* < 0.002 (Student's *t*-test).

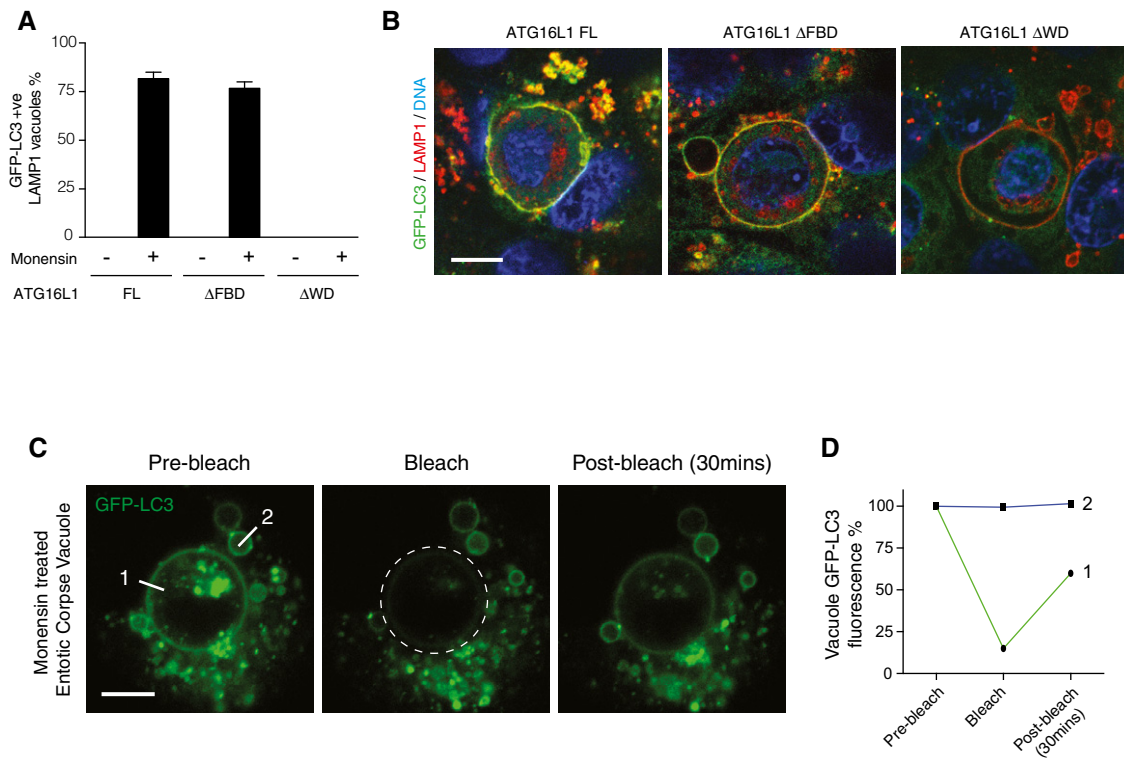


Figure EV2. Monensin-induced LC3 lipidation to entotic corpse vacuole requires the WD40 CTD of ATG16L1.

- A Quantification of GFP-LC3 recruitment to LAMP1-positive entotic corpse-containing vacuoles in MCF10A *ATG16L1*^{-/-} cells complemented full-length (FL), ΔFBD or ΔWD ATG16L1 ± monensin (100 μM, 1 h).
- B Representative confocal images of entotic corpse-containing vacuoles in GFP-expressing MCF10A cells treated with 100 μM monensin for 1 h and stained for LAMP1 (red) and DNA (blue). Scale bar: 10 μm.
- C Representative sequence images from FRAP analysis of GFP-LC3 on entotic corpse-containing vacuoles treated with monensin (100 μM, 1 h). The region marked by a broken-line circle was photobleached, and the recovery of fluorescence at line 1 and 2 was monitored. Scale bar: 10 μm.
- D Quantification of GFP fluorescence at line 1 and 2 from (C).

Data information: In (A), data are presented as mean ± SEM from three independent experiments.

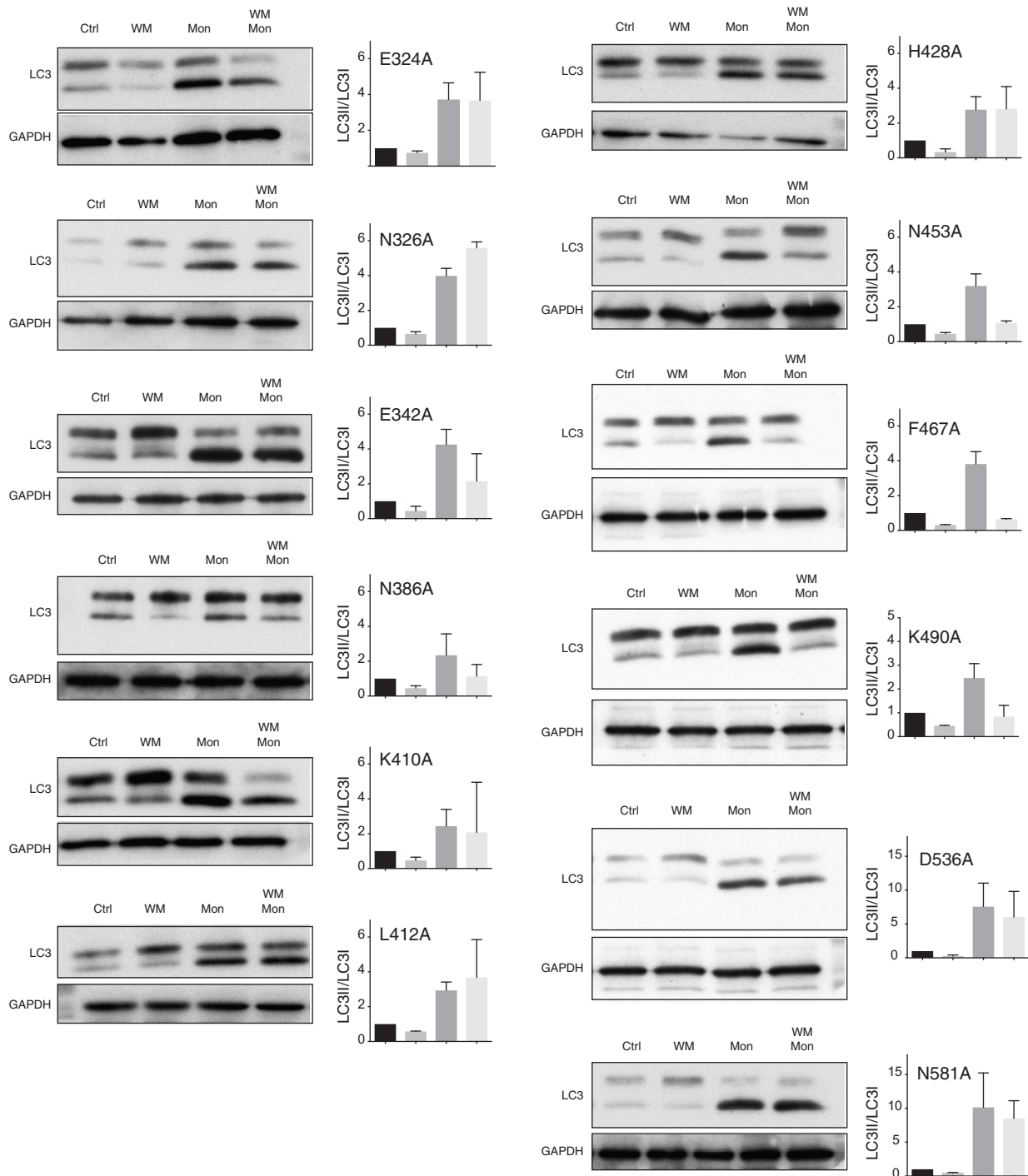


Figure EV3. Screening of ATG16L1 WD40 CTD mutants for monensin-induced non-canonical autophagy.

Western blotting of LC3 from ATG16L1-complemented HCT116 cells treated with wortmannin (WM, 67 μ M), monensin (Mon, 100 μ M) or both for 1 h. To the side is the quantification of LC3-II/LC3-I ratios. Data are presented as mean \pm SEM from three independent experiments.

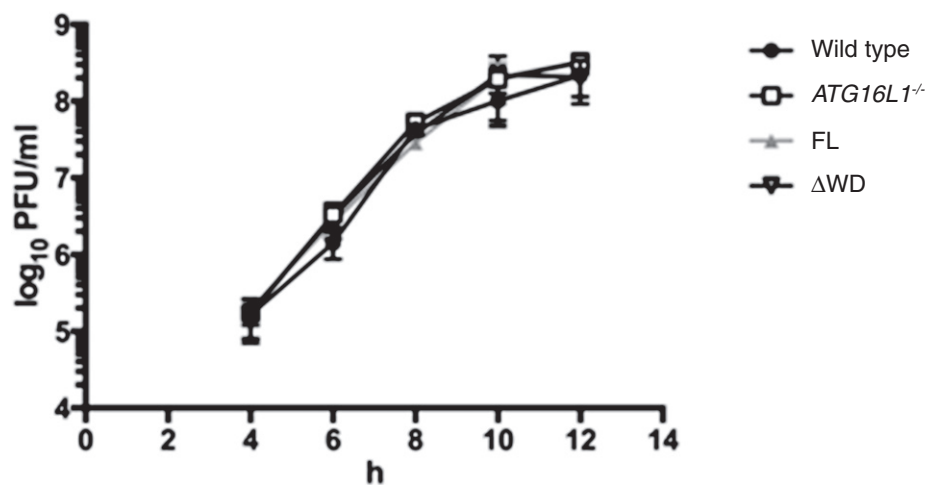


Figure EV4. The effect of ATG16L1 WD40 CTD on IAV titre.

Wild-type or *ATG16L1*^{-/-} HCT116 cells complemented with full-length (FL) or ΔWD ATG16L1 were infected with IAV PR8 at an moi of 5 PFU per cell. At the indicated timepoints, the titre of virus in the supernatant was determined by plaque assay on MDCK cells. Error bars are standard deviation from 3 replicates.

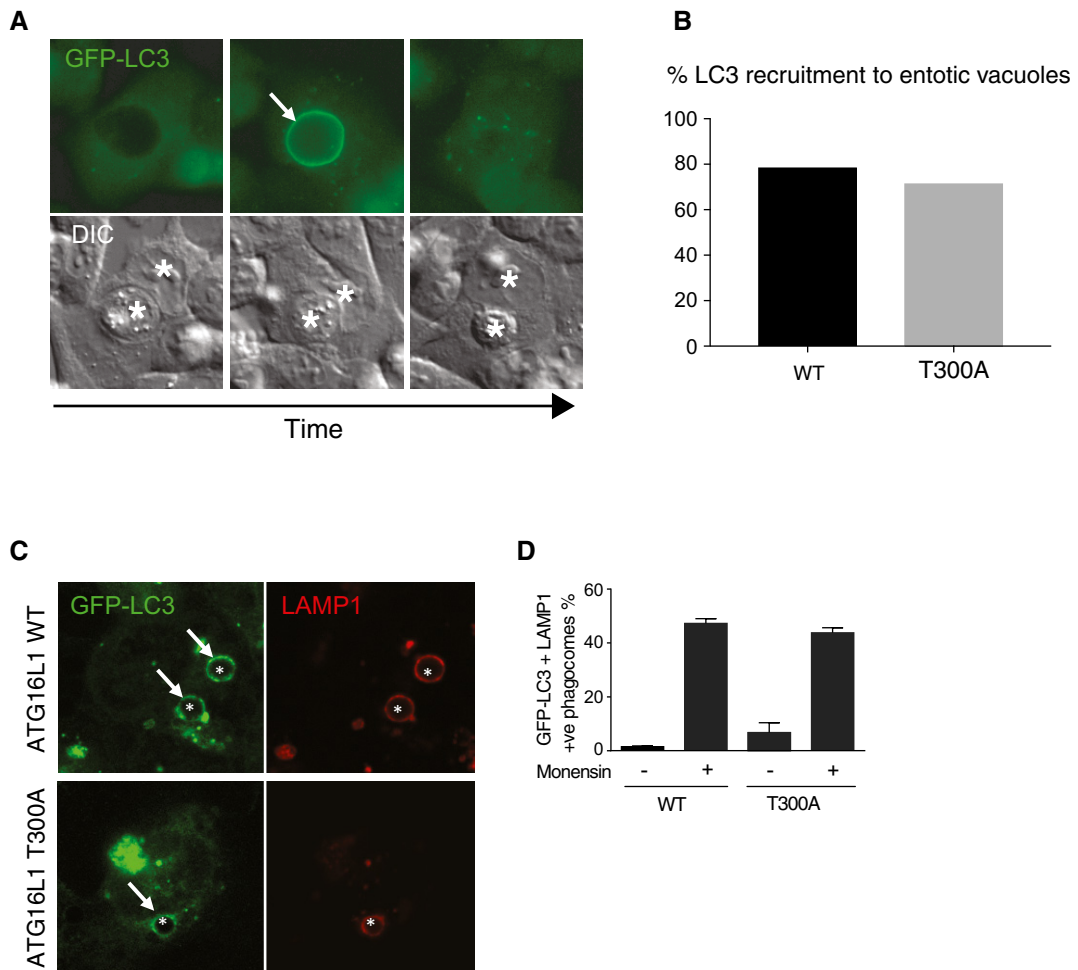


Figure EV5. ATG16L1 T300A mutation has no effect on non-canonical autophagy-associated LC3 lipidation.

A Wide-field time-lapse images showing the recruitment of GFP-LC3 to entotic vacuoles in wild-type HCT116 cell-in-cell structures. Arrow indicates GFP-LC3 recruitment to entotic vacuole. Asterisks indicate the host and internalised cells.

B Quantification of GFP-LC3 recruitment to entotic vacuoles over 20 h in wild-type and ATG16L1 T300A-expressing HCT116 cells. Data represent analysis of > 15 structures.

C Confocal images of latex bead-containing phagosomes in monensin-treated (100 μ M, 1 h) GFP-LC3-expressing HCT116 cells expressing wild-type or T300A ATG16L1. Asterisks indicate latex bead-containing phagosomes, and arrows indicate GFP-LC3-positive phagosomes.

D Quantification of GFP-LC3 recruitment to LAMP-1-positive phagosomes in wild-type and T300A HCT116 cells. 100 phagosomes were counted per experiment. Data information: In (D), data are presented as mean \pm SEM from three independent experiments.